Ordered Surface Alloy of Bulk-Immiscible Components Stabilized by Magnetism

S. Mehendale,[1] Y. Girard,[1] V. Repain,[1] C. Chacon,[1] J. Lagoute,[1] S. Rousset,[1]
Madhura Marathe,[2] and Shobhana Narasimhan[2]

[1]*Laboratoire Matériaux et Phénomènes Quantiques, Université Paris Diderot-Paris 7, UMR CNRS 7162, 75205 Paris Cedex 13, France*

[2]*Theoretical Sciences Unit, Jawaharlal Nehru Centre for Advanced Scientific Research, Jakkur, Bangalore - 560064, India*

(Received 1 May 2010; published 28 July 2010)

Using scanning tunneling microscopy and a diffraction experiment, we have discovered a new ordered surface alloy made out of two bulk-immiscible components, Fe and Au, deposited on a Ru(0001) substrate. In such a system, substrate-mediated strain interactions are believed to provide the main driving force for mixing. However, spin-polarized *ab initio* calculations show that the most stable structures are always the ones with the highest magnetic moment per Fe atom and not the ones minimizing the surface stress, in remarkable agreement with the observations. This opens up novel possibilities for creating materials with unique properties of relevance to device applications.

DOI: 10.1103/PhysRevLett.105.056101 PACS numbers: 68.55.Nq, 68.35.bd, 68.35.Md, 68.37.Ef

The development of nanostructured bimetallic alloys is a continuous challenge in many areas such as heterogenous catalysis [1], magnetic information storage [2], and even clean energy production [3]. Indeed, alloys have been valued, for their superior properties compared to the constituent elements, since ancient times. Unfortunately, many pairs of metals do not mix; for example, the magnetic metals Fe, Ni, and Co do not form stable bulk alloys with many metals, because of the large mismatch between the sizes of the constituent atoms. However, a new class of surface alloys has emerged in pioneer experiments [4,5], where bulk-immiscible components can be stabilized by the substrate-mediated strain interactions. It is generally believed that stress relief provides the driving force for mixing [6]. Accordingly, in the surface alloys of the form AB/C the intuitive choice for the substrate C has been one which has a lattice constant in between those of A and B. A few systems have been successfully investigated following this idea [5,7–9]. However, only one system, AgCu on Ru(0001), displays an atomically mixed surface alloy [5], although disordered. Very recently, considering two additional effects: (i) effective atomic sizes at surfaces which can be significantly different than in the bulk, and (ii) chemical effects, a number of systems that should display atomically mixed alloys were predicted [10], but never observed.

In this Letter, we report on one of these systems, Fe_xAu_{1-x} on a Ru(0001) substrate, which displays an atomically mixed and pseudomorphic alloy. Most importantly, we show that $Fe_{0.33}Au_{0.67}$ presents a long-range-ordered $\sqrt{3} \times \sqrt{3}$ surface-confined alloy structure, which is the first demonstration of atomic ordering in this new class of materials. Finally, we demonstrate by exhaustive *ab initio* calculations that magnetism is the driving force for the high stability of this long-range-ordered alloy structure. Since AuFe is a model system for magnetic frustration with strong exchange interactions, our work opens the way to the discovery of novel magnetic states which could have applications in storing information.

Fe-Au/Ru constitutes an ideal system for observing surface alloying, because here both chemical and elastic interactions promote mixing, and also because the effective sizes of Fe and Au *surface* atoms on a Ru(0001) surface are 2.56 and 2.90 Å, respectively [10], resulting in a mean value of 2.73 Å which matches the nearest-neighbor spacing on the Ru substrate. Further, since Fe is magnetic, this system allows us to explore questions about how alloying affects magnetism, and also the reverse question [11].

All experiments were performed in an ultrahigh vacuum system (2×10^{-10} mbar) where we cleaned our Ru(0001) single crystal by cycles of oxygen exposure at 1400 K and flashing at 1800 K. The purity of the sample was verified by obtaining vanishingly small Auger electron spectroscopy signals for carbon and oxygen impurities and sharp diffraction spots in the low energy electron diffraction (LEED) pattern. As observed by scanning tunneling microscopy (STM), the sample displayed large ~200 nm wide terraces with less than 0.01 ML of atomic carbon impurities. The alloy films were prepared by depositing one metal, annealing, and repeating the same procedure for the second metal; in this way large islands were obtained. Au was deposited from an *e*-beam heated Mo crucible at the rate of 0.04 ML/min, and Fe was deposited from an *e*-beam heated Fe rod at the rate of 0.07 ML/min. Evaporation rates were determined by analyzing the STM images [12] giving rise to a typical error bar for the concentration x of around 5%. The final results were found to be independent of whether Fe or Au was deposited first, demonstrating that we indeed reached the equilibrium configuration. It is also worth mentioning that all STM and LEED studies have been performed at room temperature.

Before co-deposition, we first considered the growth of Fe alone and Au alone on Ru(0001). Ru is a refractive material, almost completely immiscible with Au and Fe at 600 K, and with a higher surface energy; this suggests that mixing between the overlayer and substrate should be disfavored. We found that Au grows layer-by-layer, with no alloying with the substrate for annealing temperatures up to 750 K. On large islands, we observed stacking fault lines with a typical period of ~4 nm, and a herringbone-like shape, in agreement with previous work [13]. Such features were not observed when Fe was deposited on Ru(0001), suggesting that the Fe atoms occupy positions in registry with the substrate. We find that Fe can mix with the substrate, through random exchange, when the annealing temperature is higher than 700 K for 10 min. Accordingly, in our experiments on surface alloys we have limited the annealing temperature to 600 K, so that mixing with the substrate is disfavored for Fe atoms, and the substrate can thus be considered as supplying only a periodic potential on which ad-atoms sit.

The codeposition of 0.40 monolayer (ML) of Au and 0.36 ML of Fe is shown in Fig. 1(a), as a typical starting configuration. Large Au islands are surrounded by Fe dendrites, which are imaged slightly darker. Fe bilayer islands are also observed on top of Au. Figure 1(b) shows an image obtained after annealing at 600 K for 20 min, in this case for a sample with 0.53 ML of Au and 0.17 ML of Fe. The observed morphology is drastically modified after annealing, showing homogeneous islands with a faint contrast within the islands due to a surface alloy [see inset of Fig. 1(b)]. No change of contrast is found at island boundaries, indicating that segregation effects are negligible as compared to the enthalpy of mixing between Au and Fe. Figures 1(c) and 1(d) show atomic resolution STM images for two different Fe concentrations. For cases where the Fe fraction x is close to 0.33, we obtain a periodic structure as shown in Fig. 1(c). Although we can observe some local defects due to an unperfect 1:2 stoichiometry, there is relatively good long-range order (LRO), giving rise to a clear LEED diffraction pattern, which will be described in detail below (see Fig. 2). Figure 1(d) shows an STM image for a stoichiometry close to 1:1. Though no LRO can be observed, the short-range correlation between Au and Fe atoms is obviously very high with different kinds of local order coexisting. For all other studied concentrations, going from Au-rich to Fe-rich phases, no LRO has been observed in the STM images.

Figure 2 focuses on the LRO alloy found close to the 1:2 stoichiometry. In Fig. 2(a), a high resolution STM image shows a contrast of ~7 pm and a periodicity corresponding to a $\sqrt{3} \times \sqrt{3}$ structure. In the inset, the LEED pattern taken at 62 eV on a 0.7 ML of $Fe_{0.30}Au_{0.70}$ is shown and confirms this structure. At this energy, the spots corresponding to the Ru(0001) surface are observed on the screen periphery. Additional spots are clearly identified, rotated by 30°, located at a $1/\sqrt{3}$ distance as compared to the Ru spots. The width of the LEED spots indicates that the ordered phase coherence is typically of the order of 6 lattice constants, in good agreement with the density of local defects observed by STM. This structure is shown in the inset of Fig. 2(b) and is the simplest two-dimensional ordered phase on a hexagonal lattice for the 1:2 stoichiometry. The simulated constant height STM image [Fig. 2(b)] calculated from *ab initio* data strongly supports the observed structure of the alloy, showing that Fe is imaged lower than Au, in good agreement with the experiments.

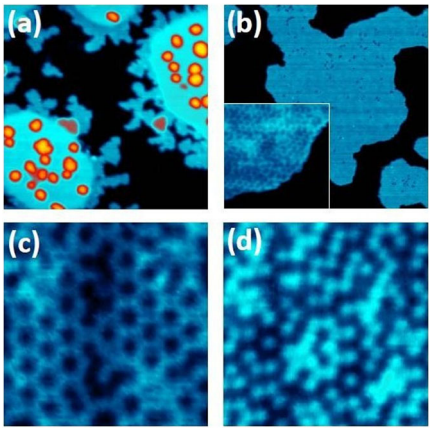

FIG. 1 (color online). STM images of (a) 50×50 nm^2 area after deposition of 0.40 ML of Au, annealed at 600 K, followed by 0.36 ML of Fe at 300 K. The large circular islands consist of Au atoms; Fe atoms grow on top of these islands (brighter small islands) and along their perimeter (slightly darker dendritic shapes). (b) 50×50 nm^2 area of a 0.7 ML coverage of a $Fe_{0.25}Au_{0.75}$ deposition, after annealing at 600 K. Inset is a zoom of 7.9×7.9 nm^2 area inside the alloyed island (c) 4×4 nm^2 area of 0.9 ML coverage of $Fe_{0.33}Au_{0.67}$ deposition, after annealing at 600 K. (d) 4×4 nm^2 area of 0.7 ML coverage of $Fe_{0.55}Au_{0.45}$ deposition, after annealing at 600 K.

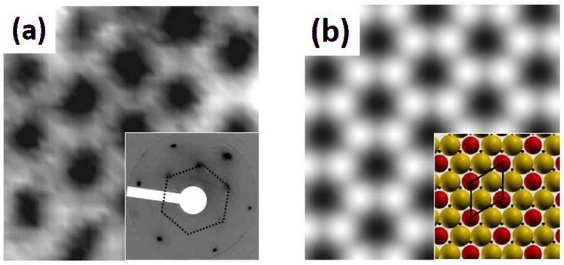

FIG. 2 (color online). The $\sqrt{3} \times \sqrt{3}$ structure of the $Fe_{0.33}Au_{0.67}$ alloy. (a) 2.1×2.1 nm^2 STM image of 0.9 ML coverage of $Fe_{0.33}Au_{0.67}$ deposition, after annealing at 600 K. The inset shows a typical negative screenshot of the LEED pattern observed at 62 eV. The hexagon connects the spots corresponding to the $\sqrt{3} \times \sqrt{3}$ unit-cell. (b) Simulated constant height STM image of the $\sqrt{3} \times \sqrt{3}$ structure, for a height of 5.7 Å and at a bias of 400 mV. Inset: atomistic model of the $\sqrt{3} \times \sqrt{3}$ structure. Black points show the positions of substrate atoms in the topmost layer, and dark (red) and bright (yellow) spheres represent Fe and Au atoms, respectively.

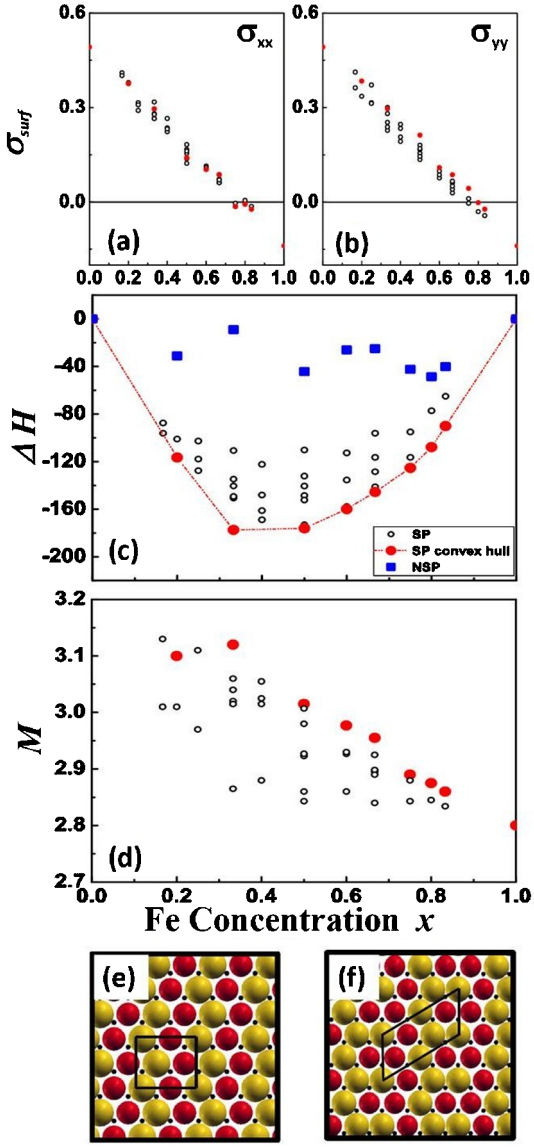

FIG. 3 (color online). Results from *ab initio* calculations for the dependence on Fe concentration x of (a) xx and (b) yy components of surface stress in eV/Å^2; (c) enthalpy of mixing ΔH in meV per atom; and (d) magnetic moment per Fe atom M in Bohr magnetons. (e) Sketch of $(2 \times \sqrt{3})$ structure for $x = 0.5$. (f) Sketch of $(2\sqrt{3} \times \sqrt{3})$ structure for $x = 0.5$. In (c), open black circles represent the results from spin-polarized (SP) calculations, SP configurations that lie on the convex hull are highlighted by filled (red online) circles, the line (red online) shows the convex hull that determines stable alloy phases, and the squares (blue online) show the results from NSP calculations for only those structures which lie on the SP convex hull. Also in (a),(b) and (d), the results for those structures that lie on the convex hull in (c) are highlighted in red. (For a more detailed description, including configurations considered, see supplementary material [20].)

In order to get a better understanding of the driving forces that stabilized these pseudomorphic alloyed phases, we have performed spin-polarized *ab initio* density functional theory calculations for several different configurations and compositions. Our calculations were performed using the QUANTUM-ESPRESSO package [14], utilizing a plane-wave basis set (with a cutoff of 20 Ry for wave functions and 160 Ry for charge densities) and ultrasoft pseudopotentials [15]. We have used a generalized-gradient approximation of the Perdew-Burke-Ernzerhof form [16] for the exchange-correlation functional. All calculations were performed using periodic boundary conditions and a slab geometry, consisting of six Ru layers, an Fe or Au or Fe-Au overlayer, and a vacuum spacing corresponding to about 17.4 Å. We have only considered configurations where the overlayer is pseudomorphic with the substrate; within this constraint, we have considered all possible configurations [17] containing two, three, four, and five atoms per unit cell, and several containing six atoms per unit cell. We have obtained optimized geometries by allowing the atoms in the overlayer, as well as the three adjacent Ru layers, to relax in all three directions. Brillouin zone sampling was performed using Monkhorst-Pack k-point grids [18] with spacing roughly equal to an (8×8) grid in the surface Brillouin zone corresponding to the smallest (1×1) unit cell for the substrate. Convergence and sampling were further improved by using the Methfessel-Paxton smearing technique [19], with the smearing width set equal to 0.05 Ry. The principal results are summarized graphically in Fig. 3, where we plot the variation in the diagonal components of the surface stress tensor σ [Figs. 3(a) and 3(b)], the enthalpy of mixing ΔH [Fig. 3(c)], and the magnetic moment M per Fe atom [Fig. 3(d)], as a function of the Fe concentration x for 43 different configurations (for a detailed description of the configurations considered, see the supplementary material [20]). With an increase in x, the stress evolves from being compressive to being tensile, following a more-or-less linear trend [see Figs. 3(a) and 3(b)]. The amplitude is found to be asymmetric around $x \sim 0.5$, as a result of the anharmonicity of interatomic potentials and the differing interatomic force constants for Fe and Au. On elastic considerations alone, this graph would imply that Fe-rich alloy phases should be favored over Au-rich ones, since the surface stress is found to go to zero at $x \sim 0.8$. However, considering the enthalpy of mixing, as seen in the black circles in Fig. 3(c), we found that the Au-rich alloy phases are favored over Fe-rich ones. Moreover, for each x, the lowest energy configuration is not the one minimizing surface stress, as highlighted by the filled (red online) circles in Figs. 3(a) and 3(b). Looking in more detail at the enthalpy of mixing, the following important conclusions can be drawn: (i) For all the structures considered by us, ΔH is found to be negative, indicating that mixing is strongly favored even though Fe and Au are bulk-immiscible. (ii) The convex hull [drawn as the filled (red online) line that passes through the filled (red online) dots] is biased towards Au-rich phases, and passes through only two structures in the Au-rich half, but five structures in the Fe-rich half. (iii) Overall, the structure with the largest

$|\Delta H|$ is the $\sqrt{3} \times \sqrt{3}$ structure for $x = 0.33$ which is indeed the phase that shows the best LRO according to STM and LEED experiments. We will call this structure "I" in the following. (iv) In the vicinity of $x = 0.33$, the data points are locally nonconvex, explaining why experiments observe I over a large compositional range. (v) At $x = 0.33$, I is considerably more stable than the other phases considered. (vi) In contrast, at other values of x, there are several nearly degenerate phases separated by only a few meV/atom. Points (ii) and (vi), taken together with entropic effects, explain why LRO is not observed for compositions further away from $x = 0.33$. For example, Figs. 3(e) and 3(f) show two ordered alloy structures for $x = 0.5$, which we find are separated by only 3 meV; a close look at the experimental alloy [Fig. 1(d)] shows indeed that these structures are locally observed, although with no long-range order. Therefore, it should be pointed out that there is a remarkable agreement between experiments and calculations.

From an inspection of our *ab initio* data, we find that for a given x, the lowest energy structure is almost always the one that maximizes the number of heteroatomic pairs and triplets, and always the one with the highest magnetic moment per Fe atom [Fig. 3(d)]. Thus, two-dimensional patterns where isolated Fe atoms are surrounded by Au atoms (as in I) are favored. This very important role of magnetism in determining the stability of surface alloys is directly demonstrated by the comparison between the enthalpies of mixing as obtained from spin-polarized (SP) and non-spin-polarized (NSP) calculations, as shown in Fig. 3(c). The blue squares that represent NSP calculations (where we have restricted ourselves to the structures that fall on the convex hull in the SP calculations) are biased towards Fe-rich phases, as one would expect from elastic considerations, and have significantly smaller values of $|\Delta H|$. In other words, magnetism has strongly promoted the mixing, and also tilts the balance towards Au-rich phases. It is also instructive to compare the Au-rich phase I with the corresponding Fe-rich phase, called II (i.e., $Fe_{0.66}Au_{0.33}$). We point out that these structures have the largest percentage (67%) of heteroatomic nearest-neighbor bonds among all the structures considered by us. It is worth pointing out that stress considerations favor II, while magnetism favors I, since [as can be seen from Fig. 3(d)] the magnetic moment per Fe atom decreases as x increases (3.12 μ_B per Fe atom in I compared to 2.96 μ_B in II). In the non-spin-polarized calculations we find that the enthalpies of mixing for I and II are, respectively, -9.02 and -25.1 meV/atom, whereas when magnetism is permitted, the corresponding values are -177.39 and -145.45 meV/atom, respectively. Note that the asymmetry between I and II has been reversed when permitting magnetism, i.e., exchange interactions are responsible for the high stability of I.

In conclusion, we have studied the two-dimensional surface alloy Fe_xAu_{1-x} on Ru(0001) by STM, LEED and *ab initio* calculations. We have found that although Fe and Au are immiscible in the bulk phase, they display commensurate alloyed phases on Ru(0001). For $x = 0.33$, we have found a long-range-ordered $\sqrt{3} \times \sqrt{3}$ phase, which is indeed the most favorable structure as calculated from first principles. We find that the primary reason for the stability of this phase is magnetism, though stress relief also plays a role. Our work opens the way to the discovery of new phases of ordered alloys on surfaces and in ultrathin films. The physical properties of these new materials, more particularly the magnetic ones, could be of interest for future applications.

We acknowledge funding from the Indo-French Centre for the Promotion of Advanced Research, the Region Ile-de-France (SESAME), and the French Ministry of Research, and helpful conversations with M. S. Narasimhan.

[1] F. Besenbacher *et al.*, Science **279**, 1913 (1998).
[2] M. L. Plummer, J. van Ek and D. Weller, *The Physics of Ultra-High-Density Magnetic Recording* (Springer, New York, 2001).
[3] V. R. Stamenkovic *et al.*, Nature Mater. **6**, 241 (2007).
[4] L. Nielsen *et al.*, Phys. Rev. Lett. **71**, 754 (1993).
[5] J. L. Stevens and R. Q. Hwang, Phys. Rev. Lett. **74**, 2078 (1995).
[6] J. Tersoff, Phys. Rev. Lett. **74**, 434 (1995).
[7] E. D. Tober *et al.*, Phys. Rev. Lett. **81**, 1897 (1998).
[8] G. E. Thayer *et al.*, Phys. Rev. Lett. **86**, 660 (2001).
[9] G. E. Thayer *et al.*, Phys. Rev. Lett. **89**, 036101 (2002).
[10] M. Marathe, M. Imam, and S. Narasimhan, Phys. Rev. B **79**, 085413 (2009).
[11] S. Blügel, Appl. Phys. A **63**, 595 (1996).
[12] I. Horcas *et al.*, Rev. Sci. Instrum. **78**, 013705 (2007).
[13] W. L. Ling *et al.*, Surf. Sci. **600**, 1735 (2006).
[14] S. Baroni *et al.*, http://www.pwscf.org/
[15] D. Vanderbilt, Phys. Rev. B **41**, 7892 (1990).
[16] J. P. Perdew, K. Burke, and M. Ernzerhof, Phys. Rev. Lett. **77**, 3865 (1996).
[17] J.-P. Serre, *Cours d'Arithmetique* (Presses Universitaires de France, Paris, 1970).
[18] H. J. Monkhorst and J. D. Pack, Phys. Rev. B **13**, 5188 (1976).
[19] M. Methfessel and A. T. Paxton, Phys. Rev. B **40**, 3616 (1989).
[20] See supplementary material at http://link.aps.org/supplemental/10.1103/PhysRevLett.105.056101.